ResearchGate

See discussions, stats, and author profiles for this publication at: https://www.researchgate.net/publication/280311938

# 2002 elvis jp014229s

**DATASET** · JULY 2015

READS
16

**3 AUTHORS**, INCLUDING:

Elvis Boes
Federal Institute of Education, Science and T…
**10** PUBLICATIONS **443** CITATIONS
SEE PROFILE

Hubert Stassen
Universidade Federal do Rio Grande do Sul
**55** PUBLICATIONS **837** CITATIONS
SEE PROFILE

Available from: Elvis Boes
Retrieved on: 01 February 2016

# A Force Field for Liquid State Simulations on Room Temperature Molten Salts: 1-Ethyl-3-methylimidazolium Tetrachloroaluminate

**Jones de Andrade, Elvis S. Böes, and Hubert Stassen***

*Grupo de Quımica Teórica, Instituto de Quımica, Universidade Federal do Rio Grande do Sul, 91540-000 Porto Alegre-RS, Brazil*

*Received: November 15, 2001; In Final Form: January 31, 2002*

A classical force field for the room temperature molten salt 1-ethyl-3-methylimidazolium tetrachloroaluminate has been developed and successfully tested against experimental data (neutron diffraction, diffusion constants) by molecular dynamics computer simulation corresponding to a temperature of 298 K. The force field parameters for the cation have been derived from the AMBER description for the protonated amino acid histidine, whereas the $AlCl_4^-$ parameters have been achieved by parametrization of intramolecular terms with van der Waals parameters taken from the literature. All atomic partial charges have been obtained from ab initio calculations using the RESP methodology.

## 1. Introduction

In recent years, a new class of solvents, generally referred to as room-temperature molten salts (RTMS) or ionic liquids, has attracted remarkable scientific activities.[1] Especially RTMS containing cationic imidazolium derivatives represent good solvents for a broad range of both, organic and inorganic materials, exhibit a high stability against strong reaction media, are immiscible in water, and are only slightly hygroscopic. Being composed of poor coordinating ions, they are broadly explored as nonvolatile solvents for a variety of reactions, including transition metal catalyzed reactions.[2]

On the other hand, only a few theoretical studies for RTMS based on the dialkylimidazolium cations have been published so far: *semiempirical* calculations of EMI·Cl directed toward the ion pair structure,[3] ab initio calculations of spectroscopic frequencies of the isolated $EMI^+$ and $AlCl_4^-$ ions,[4] and ab initio studies on the $EMI{\cdot}AlCl_4$ ion pair and its contribution to the intramolecular neutron scattering structure factor.[5] Very recently, classical condensed phase simulations on non RTMS containing the dimethylimidazolium cation have been described,[6] mainly focusing on basic equilibrium properties. To our knowledge, there are no theoretical condensed phase descriptions for RTMS containing cationic imidazolium derivatives.

In this short communication, we present a force field developed for the liquid phase of the RTMS 1-ethyl-3-methylimidazolium ($EMI^+$) tetrachloroaluminate. For this particular RTMS, experimental neutron diffraction experiments have been undertaken.[5] In addition, diffusion constants for the $EMI^+$ cation of this RTMS have been measured experimentally.[7] Thus, experimental data necessary for a force field development are available for both, the structural and dynamical features of the $EMI{\cdot}AlCl_4$ RTMS.

## 2. Methodology

Motivated by the clear guidelines[8] for the parameter development, we have chosen the AMBER force field functional form[9] for the potential energy $V$,

$$V = \sum_{\text{bonds}} k_r(r - r_{\text{eq}})^2 + \sum_{\text{angles}} k_\theta(\theta - \theta_{\text{eq}})^2 + \sum_{\text{dihedrals}} \frac{V_n}{2}(1 + \cos[n\phi - \gamma]) + \sum_{i=1}^{N-1}\sum_{j>i}^{N}\left\{4\epsilon_{ij}\left[\left(\frac{\sigma_{ij}}{r_{ij}}\right)^{12} - \left(\frac{\sigma_{ij}}{r_{ij}}\right)^{6}\right] + \frac{q_i q_j}{r_{ij}}\right\} \quad (1)$$

Here, the parameters have the usual meaning. Note that the Lennard-Jones part of the potential function as written in eq 1 differs from the original AMBER formalism $A_{ij}/r_{ij}^{12} - B_{ij}/r_{ij}^{6}$ for our computational purposes. The Lennard-Jones parameters $\epsilon_{ij}$ and $\sigma_{ij}$ between unlike atom-types have been obtained from the Lorentz−Berthelot mixing rules.[10] Polarization effects were not included, not only for computational simplicity but also due to the fact that atomic Mulliken charges of the isolated ions are very similar to those in the cation−anion complex of $EMI{\cdot}AlCl_4$.[5]

As a starting point of the force field development, we have used optimized cation and anion geometries from UHF/6-31G(d) calculations performed with the GAMESS program.[11] For both ions, the electrostatic potential (ESP) grid was generated and used to get RESP atomic charges with the one-conformation two-stage standard RESP fitting procedure performed by the RESP program of the AMBER package.[12] The obtained partial charges for $AlCl_4^-$ and the $EMI^+$ are depicted as numbers in Figure 1. Also, the lacking anion equilibrium bond lengths $r_{\text{eq}}$ and bond angles $\theta_{\text{eq}}$ have been taken from the optimized geometries.

The force field parameters for the $EMI^+$ cation (Figure 1) have been established recognizing that the imidazolium residue corresponds to the protonated amino acid histidine. By completion of the $EMI^+$ structure with the AMBER atom types[9] as depicted in Figure 1, all the van der Waals parameters, force constants, and dihedral parameters have been directly taken from the AMBER force field[9] with the exception of not defined dihedrals that were treated perfectly in accordance with the procedure outlined in ref 8.

The $AlCl_4^-$ anion's intramolecular parameters $k_r$ and $k_\theta$ have been obtained as described in ref 8. For the $k_r$ development, molecular mechanics calculations with the Tinker Software Package[13] have been carried out. The Lennard-Jones parameter for the chlorine atoms are those from ref 8, whereas the

* Corresponding author. E-mail: gullit@iq.ufrgs.br.

10.1021/jp014229s CCC: $22.00 © 2002 American Chemical Society
Published on Web 03/14/2002

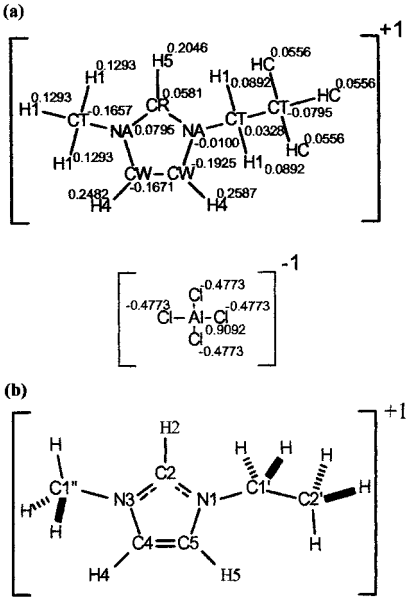


**Figure 1.** (a) Schematic structures and AMBER atom types for the $EMI^+$ cation and $AlCl_4^-$ anion. The numbers represent partial atomic charges (in units of *e*) as obtained by the RESP methodology. (b) IUPAC nomenclature for the $EMI^+$.

**TABLE 1: Force Field Parameters from Eq 1 for the $AlCl_4^-$**

| bond | $k_r$/kJ mol$^{-1}$Å$^{-2}$ | $r_{eq}$/Å |
|---|---|---|
| Al−Cl | 485.34 | 2.17 |
| **angle** | $k_\theta$/kJ mol$^{-1}$rad$^{-2}$ | $\theta_{eq}$/deg |
| Cl−Al−Cl | 209.2 | 109.5 |
| **Lennard-Jones** | $\epsilon_{ii}$/kJ mol$^{-1}$ | $\sigma_{ii}$/Å |
| Al | 1.297 | 3.911 |
| Cl | 1.109 | 3.471 |

aluminum's Lennard-Jones parameters have been taken from the DREIDING force field[14] without modification. All the anion's potential parameters are summarized in Table 1.

## 3. Simulational Details

Molecular dynamics (MD) simulations of a mixture containing 128 $EMI^+$ cations and 128 $AlCl_4^-$ anions have been performed with the MDynaMix program version 4.3.[15] The simulations were carried in the *NVT* ensemble with a Nosé−Hoover thermostat[16] maintaining a temperature of 298 K (coupling constant 30 fs). The initial configurations have been created by arranging the ions randomly mixed on a fcc lattice in a cubic box with dimensions corresponding to the experimental density of 1.302 g/cm$^3$.[5,17] Standard periodic boundary conditions and the minimum image conventions have been applied. The Tuckerman−Berne double time-step algorithm[18] was employed with long and short time-steps of 2 and 0.2 fs, respectively. All the distance dependent properties have been cut off beyond 17 Å, with the long-range electrostatic interactions corrected by the Ewald summation.[10] Lennard-Jones and Coulomb interactions involving three bonds have been reduced by factors described as default by AMBER.[9]

The equilibration of the simulations has been extended to 200 ps by monitoring carefully thermodynamic properties (total energy, pressure, potential energy contributions), molecular geometries (bond lengths and angles, dihedrals), and fluctuations in these properties. Production runs were extended at least to 100 ps. Several initial structures have been equilibrated in order to get the necessary statistical accuracy in the calculated properties. In addition to basic thermodynamic data, the mean-squared displacement[10] and all atom−atom pair distribution functions have been sampled in time intervals of 10 fs from the production runs by a modified version of the TRANAL program.[15]

**TABLE 2: Selected Angles and Its Variations during the Simulations**

| bond pairs | angle/deg |
|---|---|
| N1−C2−N3 | 109.78 ± 0.06 |
| C2−N3−C4 | 106.90 ± 0.06 |
| N3−C4−C5 | 108.05 ± 0.05 |
| C4−C5−N1 | 107.98 ± 0.05 |
| C5−N1−C2 | 106.81 ± 0.05 |
| total internal angle | 539.52 ± 0.06 |
| **main dihedrals** | **dihedral angle/degrees** |
| C2′-C1′-N1−C2 | 85.58 ± 0.68 |
| C2′-C1′-N1−C5 | 95.16 ± 0.70 |

In addition, several short *NpT* simulations have been carried out in order to establish roughly the density corresponding to the force field. The obtained values agree with the experimental density of 1.302 g/cm$^3$ [5,17] within a range of ±5%.

## 4. Results and Discussion

The intermolecular potential energy of $EMI{\cdot}AlCl_4$ from the simulations has been estimated as −252.6 ± 1.1 kJ/mol. The breakdown into van der Waals ($U_{vdw}$ = − 41.9 kJ/mol) and electrostatic contributions ($U_{el}$ = − 210.7 kJ/mol) shows the expected strong Coulombic behavior probably explaining most of the interesting properties observed in this liquid. Using the approximation of ideal vapor behavior and neglecting volume changes in the liquid phase, we calculate the enthalpy of vaporization $\Delta H_{vap}$ for the $EMI{\cdot}AlCl_4$ by

$$\Delta H_{vap} = -U + RT \tag{2}$$

producing $\Delta H_{vap}$ = 255.2 kJ/mol, clearly indicating the non-volatile character of this ionic liquid.

The analysis of the bond stretching, bending and torsional motions indicate that the $AlCl_4^-$ anion and the imidazolium residue of the $EMI^+$ cation maintain almost rigid structures. As becomes evident from some selected angles summarized in Table 2, the imidazolium ring remains planar. Dihedrals involving the aliphatic side chains move during the simulations, demonstrating that both, the ethyl and the methyl substituents are more flexible than the ring unit of the cation. The variation of only ±0.06° in the total internal angle of the ring unit illustrates its rigid character enabling a possible rigid body treatment for the imidazolium ring system.

To extract structural information from the simulation, we have computed all the atom−atom pair distribution functions $g_{ij}(r)$. Although a detailed discussion of the structural features in this RTMS will be the subject of a forthcoming publication, some results for the $EMI{\cdot}AlCl_4$ are presented here. For the deuterated isotope of this particular RTMS, an experimental pair distribution function $g_n(r)$ obtained from neutron diffraction data has been published recently.[5,19] Summing up all the atom−atom pair distributions weighted by the mole fractions $x_i$ and neutron scattering cross sections $b_i$, the experimental $g_n(r)$ has been calculated by

$$g_n(r) = \frac{\sum_{ij} x_i x_j b_i b_j g_{ij}(r)}{(\sum_i x_i b_i)^2} \tag{3}$$

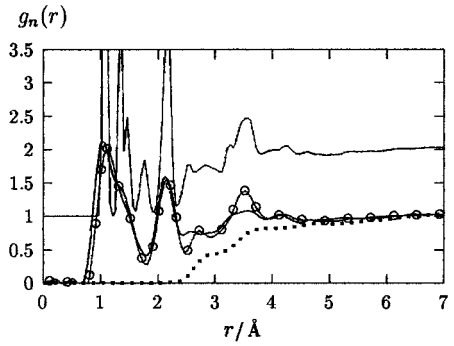


**Figure 2.** Neutron scattering pair distribution function $g_n(r)$ from eq 3 as obtained from the simulation (full line, shifted by 1) and from experiment (full line, not shifted). Also illustrated: the fast Fourier broadened simulated $g_n(r)$ (full line with ○) and the intermolecular contribution to $g_n(r)$ (dotted line).

**TABLE 3: Important Cation−Anion Distances (Å) from Quantum Mechanical Dimer Calculations[5] and from Pair Distribution Functions of the Present Work**

| atom pair | ref 5 | this work |
|---|---|---|
| H2−Cl | 2.67 | 2.78 |
| H4−Cl | | 2.83 |
| H5−Cl | | 2.83 |
| $H_{C1''}$−Cl | 3.05 | 2.98 |
| $H_{C1'}$−Cl | 2.94−3.22 | 2.93 |

The $g_n(r)$ from the simulation is compared with the experimental $g_n(r)$ in Figure 2. It becomes evident that peak positions in the simulated $g_n(r)$ agree very well with the experimental peak position. Moreover, smoothing the simulated $g_n(r)$ slightly by fast Fourier techniques, a remarkable agreement between simulated and experimental $g_n(r)$ has been achieved, not only for the peaks position but also for their shapes and amplitudes. Note that all the distances below 2 Å correspond to intramolecular contributions. The first intermolecular peak positions determined from the simulated $g_{ij}(r)$ are listed in Table 3 and are coordinated to hydrogen-chloro pairs with distances between 2.78 and 2.98 Å. A difference between experimental and simulated $g_n(r)$ is found in the range between 3.6 and 3.8 Å, where the simulated $g_n(r)$ presents a maximum with significantly amplitude that cannot be found in the experimental results. This particular peak has been traced back to intra- and intermolecular pair distribution functions involving chloro atoms with Cl−Cl pairs representing the principal contribution. A possible explanation for the difference between experiment and simulation in this region of the $g_n(r)$ might be related to the experimentally observed formation of clusters (like $Al_2Cl_7^-$, $Al_3Cl_{10}^-$, etc.) in molten chloroaluminates.[20]

In Figure 2, we have also included the intermolecular contribution (not broadened by fast Fourier transformation) to $g_n(r)$ from the simulations. This pair distribution function contains small amplitudes below 2.5 Å, with several H−Cl pairs (see Table 3) creating a plateau at approximately 3 Å. We observe differences between the total $g_n(r)$ and its intermolecular contribution up to distances beyond 6 Å. In addition, comparing total and intermolecular $g_n(r)$, one can conclude that all the structural features in the total $g_n(r)$ are originated at intramolecular distances.

Finally, to get some insight into the dynamical features of the presented force field, we have computed the diffusion constants for the $EMI^+$ cation and the $AlCl_4^-$ anion from the slope in the mean-squared displacements of these species. The calculated diffusion constants, $1.16 \times 10^{-6}$ and $0.96 \times 10^{-6}$ $cm^2/s$ for $EMI^+$ and $AlCl_4^-$, respectively, are an order of magnitude smaller than for most liquids. In the case of $EMI^+$, an experimental diffusion constant of $0.95 \times 10^{-6}$ $cm^2/s$ has been elucidated from NMR data.[7] Comparing the simulated diffusion coefficient with the experimental finding, one might conclude that the proposed force field for $EMI{\cdot}AlCl_4$ is also able to give a reasonable insight into the dynamical features of this RTMS.

**Acknowledgment.** Financial support from the Brazilian agencies CNPq (process 521628/97-0) and FAPERGS (process AUX 00/0902.7) as well as a grant (J.d.A.) from the CAPES are gratefully acknowledged. We thank J. Caldwell and M. Froeyen for their assistance on RESP charge fitting from GAMESS results as well as A. Laaksonen and A. P. Lyubartsev for providing MDynaMix and TRANAL with the necessary start up assistance. Fruitful and stimulating discussions with J. Dupont and P.A. Netz also have contributed significantly to the present work.

## References and Notes

(1) Welten, T. *Chem. Rev.* **1999**, *99*, 2071.
(2) Dupont, J.; Consorti, C. S.; Spencer, J. *J. Braz. Chem. Soc.* **2000**, *11*, 337. Wasserscheid, P.; Keim, W. *Angew. Chem., Int. Ed. Engl.* **2000**, *39*, 3772.
(3) Dymek, Jr.; Stewart, J. J. P. *Inorg. Chem.* **1989**, *28*, 1472.
(4) Takahashi, S.; Curtiss, L. A.; Gosztola, D.; Koura, N.; Saboungi, M. L. *Inorg. Chem.* **1995**, *34*, 2990.
(5) Takahashi, S.; Suzuya, K.; Kohara, S.; Koura, N.; Curtiss, L. A.; Saboungi, M. L. *Z. Phys. Chem.* **1999**, *209*, 209.
(6) Hanke, C. H.; Price, S. L., Lynden-Bell, R. M. *Mol. Phys.* **2001**, *99*, 801.
(7) Larive, C. K.; Lin, M.; Piersma, B.; Carper, W. R. *J. Phys. Chem.* **1995**, *99*, 9, 12400; Carper, W. R.; Mains, G. J.; Piersma, B. J.; Mansfield, S. L.; Larive, C. K. *J. Phys. Chem.* **1996**, *100*, 4724.
(8) Fox, T.; Kollman, P. A. *J. Phys. Chem. B* **1998**, *102*, 8070.
(9) Cornell, W. D.; Cieplak, P.; Bayly, C. I.; Gould, I. R.; Merz., K. M., Jr; Ferguson, D. M.; Spellmeyer, D. C.; Fox, T.; Caldwell, J. W.; Kollman, P. A. *J. Am. Chem. Soc.* **1995**, *117*, 5179.
(10) Allen, M. P.; Tildesley, D. J. *Computer Simulation of Liquids*; Clarendon Press: Oxford, U.K., 1987.
(11) Schmidr, M. W.; Baldridge, K. K.; Boatz, J. A.; Elbert, S. T.; Gordon, M. S.; Jensen, J. J.; Koseki, S.; Matsunaga, N.; Nguyen, K. A.; Su, S.; Windus, T. L.; Dupuis, M.; Montgomery, J. A. *J. Comput. Chem.* **1993**, *14*, 1347.
(12) Case, D. A.; Pearlman, D. A.; Caldwell, J. W.; Cheatham, T. E., III; Ross, W. S.; Simmerling, C. L.; Darden, R. A.; Merz, K. M.; Stanton, R. V.; Cheng, A. L.; Vincent, J. J.; Crowley, M.; Tsui, V.; Radmer, R. J.; Duan, Y.; Pitera, J.; Massova, I.; Seibel, G. L.; Singh, U. C.; Weiner, P. K.; Kollman, P. A. *AMBER 6*; University of California: San Francisco, 1999.
(13) Pappu, R. V.; Hart, R. K.; Ponder, J. W. *J. Phys. Chem. B* **1998**, *102*, 9725. Dudek, M. J.; Ramnarayan, K.; Ponder, J. W. *J. Comput. Chem.* **1998**, *19*, 548.
(14) Mayo, S. L.; Olafson, B. D.; Goddard, W. A., III. *J. Phys. Chem.* **1990**, *94*, 8897.
(15) Lyubartsev, A. P.; Laaksonen, A. *Comput. Phys. Comm.* **2000**, *128*, 565.
(16) Nosé, S. *Mol. Phys.* **1984**, *52*, 525.
(17) Fannin, A. A.; Floreani, D. A., Jr.; King, L. A.; Landers, J. S.; Piersma, B. J.; Stech, D. J.; Vaughn, R. L.; Wilkes, J. S.; Williams, J. L. *J. Phys. Chem.* **1984**, *88*, 2614.
(18) Tuckerman, M.; Berne, B. J. *J. Chem. Phys.* **1992**, *97*, 1990.
(19) Saboungi, M. L.; Kohara, S. Private communication.
(20) Tosi, M. P.; Price, D. L.; Saboungi, M. L. *Annu. Rev. Phys. Chem.* **1993**, *44*, 173; Akdeniz, Z.; Tosi, M. P. *Z. Naturforsch. A* **1999**, *54*, 180.